Crystal structure of dicalcium chromate hydrate

C. E. Botez[a] and P. W. Stephens
Department of Physics and Astronomy, State University of New York at Stony Brook, Stony Brook, New York, 11794-3800 and National Synchrotron Light Source, Brookhaven National Laboratory, Upton, New York 11973

Oladipo Omotoso
Natural Resources Canada, Energy Technology Centre, Devon, Alberta, T9G 1A8, Canada

(Received 8 September 2003; accepted 9 December 2003)

Direct methods and Rietveld analysis were applied to high-resolution synchrotron X-ray powder diffraction data to solve the crystal structure of dicalcium chromate hydrate ($Ca_2CrO_5 \cdot 3H_2O$). The compound crystallizes in monoclinic symmetry (space group Cm, $Z=2$), with $a=8.23575(5)$ Å, $b=7.90302(4)$ Å, $c=5.20331(3)$ Å, and $\beta=98.0137(3)°$. The structure is built from double-layers of CrO_4 tetrahedra and CaO_8 polyhedra that run parallel to the (001) plane. © *2004 International Centre for Diffraction Data.* [DOI: 10.1154/1.1648316]

I. INTRODUCTION

The occupational and environmental health hazards associated with chromium date back to the 1920s, when it was first observed that the lung cancer rate among the workers in the German chromium processing industry was noticeably higher than that of the general population (Langard, 1990). Since then, extensive environmental, chemical, and medical research has led to significant progress in the understanding of different aspects of chromium contamination. It is known, for example, that trivalent chromium (Cr^{III}) compounds are generally insoluble, whereas hexavalent chromium (Cr^{VI}) forms soluble compounds, and thus has the ability to penetrate through cell membranes, mainly because of the chemical similarity of CrO_4^{-2} to phosphate, which is transported into all cells. Once in the cell Cr^{VI} is transformed into Cr^{III}, which, in turn, can induce different types of genetic damage (Qi *et al.*, 2000). It is also well established that the most damaging ingestion pathway for Cr^{VI} is inhalation (Langard, 1990) and, consequently, Cr^{VI}-contaminated wastes should not be incinerated. Another method of disposing of such wastes would be to place them in landfills, but, in time, they are likely to leach and may contaminate ground water resources. A better solution is to contain the wastes in ordinary Portland cement, where heavy-atom contaminants are typically immobilized in a high-strength monolithic cement-waste matrix. Depending on the type of the metal ions, stabilization can be through chemisorption, precipitation, chemical incorporation in the hydrated cement phases, physical entrapment, or a combination of these (Glasser, 1993; Means *et al.*, 1995). Cr^{VI} contaminants added to Portland cement are known to be very mobile, except when additives are mixed with the cement paste to reduce Cr^{VI} to Cr^{III} (Kindness *et al.*, 1994). Typically, when Cr^{VI} solution is added to Portland cement, soluble $CaCrO_4 \cdot 2H_2O$ forms within the first day of reaction. However, as more calcium comes into the pore solution from dissolution of the tricalcium silicate component of Portland cement, the new stable product is $Ca_2CrO_5 \cdot 3H_2O$. In the cement–Cr^{VI} waste matrix, $Ca_2CrO_5 \cdot 3H_2O$ is formed according to (Omotoso *et al.*, 1998a, b)

$$Ca(OH)_2 + CaCrO_4 \cdot 2H_2O \rightarrow Ca_2CrO_5 \cdot 3H_2O. \quad (1)$$

This compound persists throughout the hydration period, *and its solubility ultimately determines the mobility of* Cr^{VI} *in a cement-waste matrix*. In this respect, understanding the crystal structure of $Ca_2CrO_5 \cdot 3H_2O$ is of major interest, since it can be used to make predictions on solubility-related phenomena, such as the incongruent dissolution of Ca and Cr ions in $Ca_2CrO_5 \cdot 3H_2O$, recently observed in standard leaching tests (Omotoso *et al.*, 1998, b).

In this paper we present the structure determination of $Ca_2CrO_5 \cdot 3H_2O$ from synchrotron X-ray powder diffraction data collected on a sample containing two phases: the main ($Ca_2CrO_5 \cdot 3H_2O$) phase and an impurity ($Ca(OH)_2$) phase, whose structure is known. We first performed a Le Bail fit (Le Bail *et al.*, 1988) to the main phase, simultaneously with a Rietveld refinement of the impurity phase, in order to extract the integrated intensities of the former. These were subsequently used as input for the direct methods structure-determination program SIRPOW (Altomare *et al.*, 1994). Eventually, the structure provided by SIRPOW was refined using the program package GSAS (Larson and Von Dreele, 1987).

II. EXPERIMENTAL DETAILS

To produce $Ca_2CrO_5 \cdot 3H_2O$, analytical grade calcium carbonate obtained from Fisher Scientific™ was ground to less than 5 μm in a micronizing mill and calcined at 950 °C. The resulting calcium oxide was slurried with de-ionized water in an inert atmosphere to prevent carbonation. The calcium hydroxide slurry produced was reacted with 1 M CrO_3 solution (Ca:Cr=2) according to

$$2Ca(OH)_2 + CrO_3 + H_2O \rightarrow Ca_2CrO_5 \cdot 3H_2O. \quad (2)$$

The slurry was filtered through a 0.45 μm cellulose acetate membrane and washed with de-ionized water. The filtered residue was dried over a dessicant in an inert atmosphere, and its density was measured using the ASTM helium pycnometer method (ASTM D2638-91, 1997).

Diffraction data were collected on the SUNY X3B1 High-Resolution Powder Diffraction Beamline at the National Synchrotron Light Source, from a sample contained in

[a] Electronic mail: botez@bn1.gov

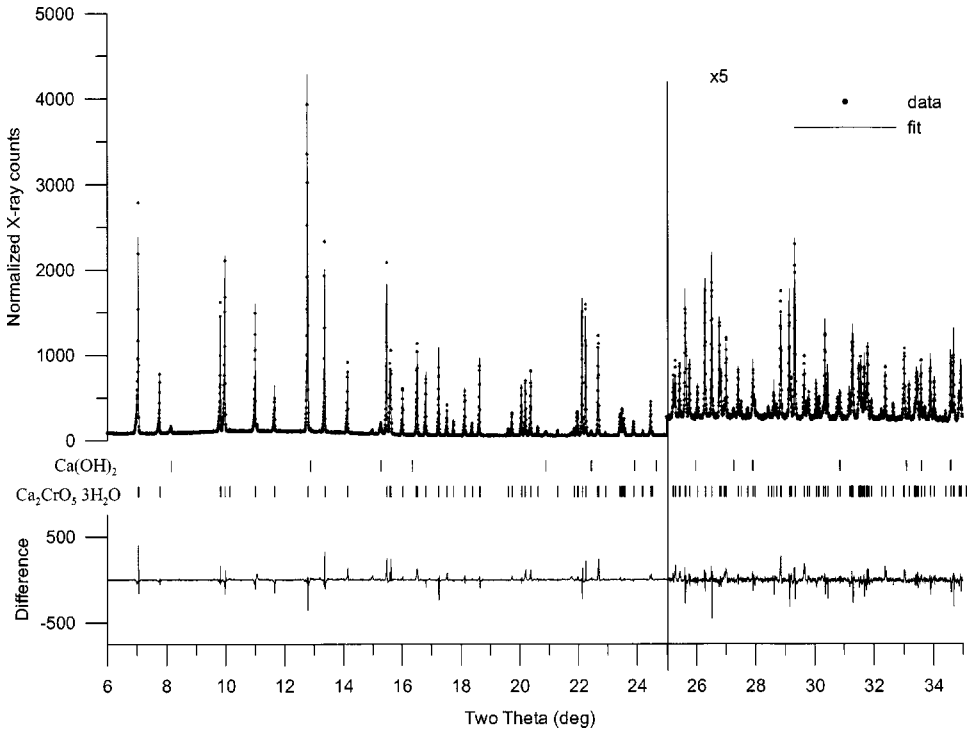

Figure 1. Two-phase [$Ca_2CrO_5 \cdot 3H_2O$ and $Ca(OH)_2$] best Rietveld refinement: the closed symbols represent the scattered intensity as a function of the angle 2θ, while the line represents the calculated pattern. The lower trace is the difference between the observed and the calculated patterns and the vertical bars are the Bragg-reflection markers for the two phases.

a 0.5-mm-diam glass capillary. X-rays of wavelength 0.6995 Å, selected by a double-crystal monochromator, were used. The wavelength and the "zero" of the diffractometer were determined with a NIST1976 corrundum standard. During the measurement, the intensity of the incoming beam was monitored by an ion chamber and normalized for the decay of the primary beam. The beam diffracted from the sample was analyzed by a Ge(111) crystal before being measured by a Na(Tl)I scintillation detector. The powder diffraction pattern was recorded at room temperature, over a 2θ angular range between 6 and 35° ($d = 1.16$ Å). Counting time was 6 s at each 0.005° 2θ step. During data collection, the capillary containing the sample was spun around its longitudinal axis perpendicular to the direction of the main beam.

III. STRUCTURE DETERMINATION AND DISCUSSION

The powder diffraction pattern includes reflections from the main $Ca_2CrO_5 \cdot 3H_2O$ phase, as well as from the impurity $Ca(OH)_2$ phase. Since the structure of calcium hydroxide is known, the low-angle reflections belonging to each phase could be separated for indexing purposes. Then, the angular positions of the first 20 reflections from the dicalcium chromate phase were accurately determined by fitting the corresponding peak profile and input into the auto-indexing program ITO (Visser, 1969). The indexing yielded a monoclinic unit cell for $Ca_2CrO_5 \cdot 3H_2O$ with a figure of merit of 80. The same cell was obtained with both trial indexing (TREOR—Werner *et al.*, 1985) and successive dichotomy (DICVOL—Boultif and Louer, 1991). The possible space groups, $C2$, $C2/m$, and Cm, were then determined from systematic-absences considerations. The number of formula units/unit cell (Z) was found using the measured density and the unit cell volume. A two-phase LeBail fit using the program FULLPROF (Rodriguez-Carvajal, 1990), allowed the extraction of 125 integrated intensities (up to 34.95° in 2θ), corresponding to as many Bragg reflections for the main $Ca_2CrO_5 \cdot 3H_2O$ phase.

The integrated intensities, together with the unit cell information, were input into the direct-methods structure determination program SIRPOW. SIRPOW runs were performed using each of the allowed space groups. No satisfactory solution was found for $C2$ ($R_w(f) = 0.118$) and $C2/m$ ($R_w(f) = 0.279$), while switching to Cm dramatically reduced the R-factor ($R_w(f) = 0.044$), suggesting that this space group is associated with the correct solution. Here, the R-factor is given by

$$R_w(f) = \frac{\Sigma(|F_o - F_c| \times F_o^2)}{\Sigma(|F_o| \times F_o^2)}, \qquad (3)$$

where F_o and F_c are the observed and the calculated structure factors, respectively, and the summation is over all the 125 Bragg reflections from dicalcium chromate.

The program package GSAS was used to refine the best structure provided by SIRPOW—the final two-phase [$Ca_2CrO_5 \cdot 3H_2O$ and $Ca(OH)_2$] Rietveld refinement is shown in Figure 1. For the dicalcium chromate phase we allowed the variation of the following quantities: the nonhydrogen atoms coordinates, isotropic thermal parameters, profile parameters, unit cell parameters, and weight fractions. No restraints were used. For the impurity phase we only refined the unit cell and the profile parameters. A pseudo-Voigt convoluted with an asymmetry function (Finger *et al.*, 1994) was used to model the peak profiles. The results of the best Rietveld refinement are shown in Table I. It should be emphasized that the estimated standard deviations (ESDs) listed are *statistical estimates*, which are valid under the assumption that the only difference between the derived model and physical reality is in the experimental counting statistics. Also worthy of note is the small weight fraction of calcium

TABLE I. Crystallographic data and details of the Rietveld refinement.

	$Ca_2CrO_5 \cdot 3H_2O$		$Ca(OH)_2$
Crystallographic data			
Space group	*C m*		*P−3m1*
a(Å)	8.23575(5)		3.59313(3)
b(Å)	7.90302(4)		3.59313(3)
c(Å)	5.20331(3)		4.9123(6)
α(°)	90		90
β(°)	98.0137(3)		90
γ(°)	90		120
V(Å^3)	335.362		54.924
Measured ρ(g cm^{-3})		2.561(2)	
Calculated ρ(g cm^{-3})	2.576		2.240
Rietveld refinement details			
Weight fractions (%)	97.5		2.5
No. of reflections	125		21
No. of refined parameters	28		5
R_B	0.0519		0.1166
λ(Å)		0.6995	
$(\sin\theta/\lambda)_{max}$(Å^{-1})		0.4298	
Step length (°)		0.005	
R_p		0.063	
R_{wp}		0.085	
χ^2		6.98	

hydroxide (2.5%). The refinement is stable with 33 parameters varying simultaneously and has figures of merit $R_{wp} = 0.085$ and $\chi^2 = 6.98$. No preferred orientation effects were observed.

Table II shows the fractional coordinates of the nonhydrogen atoms for the two phases. Several attempts were made at finding the missing hydrogens using Fourier difference maps, but they could not be unambiguously located, most likely because of the presence of the much heavier Cr and Ca atoms. The three-dimensional (3D) structure of $Ca_2CrO_5 \cdot 3H_2O$ is shown in Figure 2. It consists of double layers (CrO_4 tetrahedra and CaO_8 polyhedra) that run parallel to the (001) face of the unit cell. Within each double layer, the distance between the Ca and the Cr planes is 3.0858 Å. Each chromium atom is coordinated with four oxygen atoms, forming tetrahedra whose O1–O3–O1 base is

TABLE II. Fractional atomic coordinates for $Ca_2CrO_5 \cdot 3H_2O$ and $Ca(OH)_2$. Numbers in parentheses are statistical estimated standard deviations from the Rietveld fit.

	X	*Y*	*Z*	*U*iso
Fractional coordinates ($Ca_2CrO_5 \cdot 3H_2O$)				
Cr1	0.1780(3)	0.000	0.3237(5)	0.0108(7)
Ca1	0.8090(3)	0.2358(2)	−0.0774(5)	0.0090(6)
O1	0.0689(6)	−0.1741(5)	0.2258(9)	0.0059(7)
O2	0.2095(8)	0.000	0.6415(11)	0.0059(7)
O3	0.3493(7)	0.000	0.1962(11)	0.0059(7)
O4	0.7417(8)	0.000	0.2096(11)	0.0059(7)
O5	0.5386(6)	0.1562(6)	−0.2740(8)	0.0059(7)
O6	0.8691(7)	0.000	−0.3243(11)	0.0059(7)
Fractional coordinates ($Ca(OH)_2$)				
O1	0.333	0.666	0.766	0.0144
H1	0.333	0.666	0.574	0.0144
Ca1	0.000	0.000	0.000	0.0144

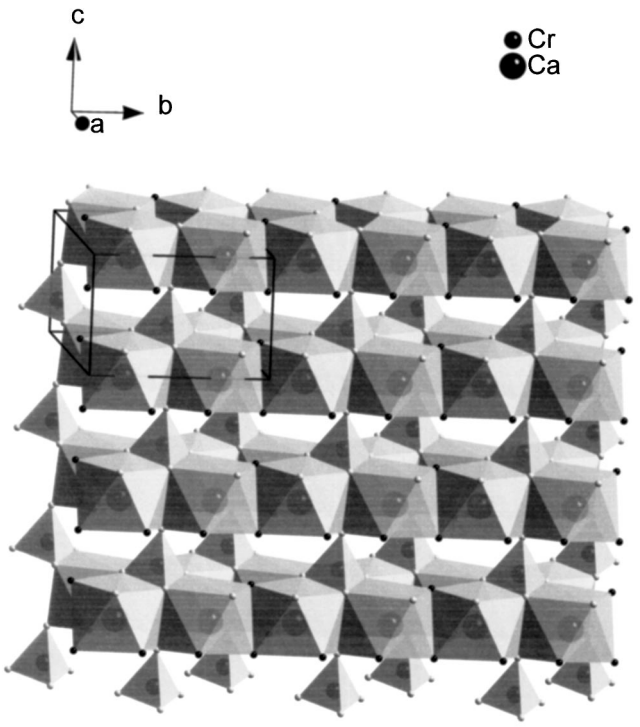

Figure 2. 3D structure of $Ca_2CrO_5 \cdot 3H_2O$, highlighting the CrO_4 tetrahedra and the CaO_8 polyhedra.

oriented (quasi)-parallel to the (001) face of the unit cell. Table III(a) shows the values of the Cr–O bond lengths and O–Cr–O bond angles that define the CrO_4 tetrahedra.

The coordination sphere of Ca, including the values of the Ca–O bond lengths, is shown in Figure 3. Oxygens O4,

TABLE III. Selected bond lengths and bond angles and torsion angles in the (a) CrO_4 tetrahedra and (b) CaO_8 polyhedra. Numbers in parentheses are statistical ESD values derived from the Rietveld refinement.

(a)	CrO_4 tetrahedra	Bond lengths (Å)
	Cr1–O1	1.683(5)
	Cr1–O2	1.638(6)
	Cr1–O3	1.640(7)
	CrO_4 tetrahedra	Bond angles (°)
	O1–Cr1–O2	108.0(2)
	O1–Cr1–O3	109.3(2)
	O2–Cr1–O3	112.6(3)
(b)	CaO_8 polyhedra	Bond lengths (Å)
	Ca1–O1	2.788(5)
	Ca1–O2	2.499(5)
	Ca1–O3	2.523(5)
	Ca1–(H)O4	2.499(5)
	Ca1–(H)O5	2.402(5)
	Ca1–(H)O6	2.355(4)
	CaO_8 polyhedra	Bond angles (°)
	O1–Ca1–O2	85.47(2)
	O2–Ca1–O3	70.20(2)
	O1–Ca1–O3	61.14(2)
	(H)O4–Ca1–(H)O5	77.8(2)
	(H)O5–Ca1–(H)O6	79.2(2)
	(H)O4–Ca1–(H)O6	79.4(2)

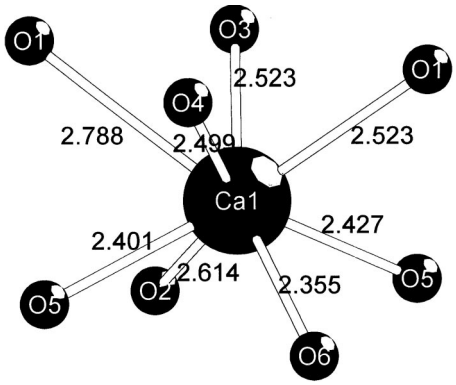

Figure 3. Coordination of Ca within the CaO_8 polyhedra.

O5, and O6 correspond to the water molecules and are coordinated with calcium atoms as hydroxyls, whose presence was previously verified by infrared OH stretching vibrations (Omotoso *et al.*, 1998a, b). The presence of Ca–O(H) bonds might explain the incongruent dissolution of dicalcium chromate, since these bonds are preferentially attacked by the acetic acid used in the Toxicity Characteristic Leaching Procedure (EPA 51, 21685, 1983). Accordingly, the leachate was observed to have a calcium to chromium mole ratio of 3.3 at an equilibrium *p*H of 12.3 (Omotoso *et al.*, 1998, b). Table III(b) shows the values of selected bond lengths and bond angles in the CaO_8 polyhedra. We note that the average values of the Ca–O(H) bond lengths and (H)O–Ca–O(H) bond angles obtained in our Rietveld refinement are 2.418 Å and 78.8°, respectively. These distances and angles, as well as the ones that define the CrO_4 tetrahedra, are in very good agreement with the ones in the literature (Bars *et al.*, 1977). We also find that the Cr atoms, and four oxygens (O2, O3 coordinated with Cr, and O4, O6 coordinated with Ca), sit on special (x,0,z) positions, on the mirror plane parallel to the (010) face of the unit cell.

ACKNOWLEDGMENTS

Research was carried out at the National Synchrotron Light Source (Brookhaven National Laboratory), which was supported by the US Department of Energy (DOE), Division of Material Sciences and Division of Chemical Sciences. The SUNY X3 beamline was supported by the DOE, under Contract No. DE-FG02-86ER45231.

Altomare, A., Cascarano, G., Giacovazzo, C., Guagliardi, A., Burla, M. C., Polidori, G., and Camalli, M. (**1994**). ''SIRPOW92—a program for automatic solution of crystal structures by direct methods optimized for powder data,'' J. Appl. Crystallogr. **27**, 435–436.

ASTM D2638-91 (**1997**). ''Standard test method for real density of calcined petroleum coke by helium pycnometer,'' American Society for Testing and Materials.

Bars, O., Le Marouille, J. Y., and Grandjean, D. (**1977**). ''Etude de chromates, molybdates et tungstates hydrates. II. Etude structurale de $CaCrO_4$ H_2O,'' Acta Crystallogr., Sect. B: Struct. Crystallogr. Cryst. Chem. **B33**, 3751–3755.

Boultif, A. and Louer, D. (**1991**). ''Indexing of powder diffraction for low symmetry lattices by the successive dichotomy method,'' J. Appl. Crystallogr. **24**, 987–993.

EPA (**1983**). ''Toxicity Characteristic Leaching Procedure,'' Environmental Protection Agency Federal Register Vol. 51, 21685.

Finger, L. W., Cox, D. E., and Jephcoat, A. P. (**1994**). ''Correction for powder diffraction peak asymmetry due to axial divergence,'' J. Appl. Crystallogr. **27**, 892–900.

Glasser, F. P. (**1993**). *Proceedings of the Chemistry and Microstructure of Solid Waste Forms* (Lewis, Boca Raton, FL), p. 1.

Kindness, A., Macia, S. A., and Glasser, F. P. (**1994**). ''Immobilization of chromium wastes in cement matrices,'' Waste Manage. Res. **14**, 3–11.

Langard, S. (**1990**). ''One hundred years of chromium and cancer: A review of epidemiological evidence and related case reports,'' Am. J. Ind. Med. **17**, 189–215.

Larson, A. C. and Von Dreele, R. B. (**1987**). ''Program GSAS, General Structure Analysis System,'' Los Alamos National Laboratory Report No. LA-UR-86-784, Los Alamos. Program and documentation available from http://public.lanl.gov/gsas.

Le Bail, A., Duro, H., and Fourquet, J. L. (**1988**). ''The ab-initio structure determination of lithium antimony tungstate ($LiSbWO_6$) by X-ray powder diffraction,'' Mater. Res. Bull. **23**, 447–452.

Means, J. L., Smith, L. A., Nehrig, K. L. W., Brauning, S. E., Gavaskar, A. R., Sass, B. M., Wiles, C. C., and Mashni, C. I. (**1995**). *The Application of Solidification/Stabilization to Waste Materials* (Lewis, Boca Raton, FL).

Omotoso, O., Ivey, D. G., and Mikula, R. J. (**1998a**). ''Hexavalent chromium in tricalcium silicate. I. Quantitative X-ray diffraction analysis of crystalline products,'' J. Mater. Sci. **33**, 507–513.

Omotoso, O., Ivey, D. G., and Mikula, R. J. (**1998b**). ''Hexavalent chromium in tricalcium silicate. II. Effects of chromium (VI) on the hydration of tricalcium silicate,'' J. Mater. Sci. **33**, 515–522.

Qi, W., Reiter, R. J., Tan, D.-X., Garcia, J. J., Manchester, L. C., Karbownik, M., and Calvo, J. R. (**2000**). ''Chromium(III)-induced 8-hydroxydeoxyguanosine in DNA and its reduction by antioxidants: Comparative effects of melatonin, ascorbate, and vitamin E,'' Environ. Health Perspect. **108**, 399–402.

Rodriguez-Carvajal, J. (**1990**). ''FULLPROF, a program for Rietveld refinement and pattern matching analysis,'' Abstracts of the Powder Diffraction Meeting, Toulouse, France, pp. 127–128. Program and documentation available from http://www-llb.cea.fr/fullweb/fullprof.htm.

Visser, J. W. (**1969**). ''A fully automatic program for finding the unit cell from powder data,'' J. Appl. Crystallogr. **2**, 89–95.

Werner, P. E. (**1985**). ''TREOR, a semi-exhaustive trial and error powder indexing program for all symmetries,'' J. Appl. Crystallogr. **18**, 367–370.